Trop J Nat Prod Res, September 2022; 6(9): ISSN 2616-0684 (Print)
ISSN 2616-0692 (Electronic)

Tropical Journal of Natural Product Research

Available online at https://www.tjnpr.org

Original Research Article

Synthesis, *In vitro*, and *In silico* Studies of Methyl Eugenol Derivatives for *Plasmodium falciparum* Inhibitor

Lucy Arianie[1]*, Muhammad I. Supriatna[1], Nuryamin Kazal[1], Nashi Widodo[2], Warsito Warsito[1], Elvina D. Iftitah[1]

[1]*Department of Chemistry, Faculty of Science, Brawijaya University, Malang, Indonesia*
[2]*Department of Biology, Faculty of Science, Brawijaya University, Malang, Indonesia*

ARTICLE INFO

Article history:
Received 07 June 20022
Revised 12 July 2022
Accepted 22 September 2022
Published online ****

ABSTRACT

Multidrug treatment has been piloted for *Plasmodium falciparum* malaria infection; however, multidrug resistance requires serious attention. Therefore, new antimalarial studies have been intensively carried out, including research on new compounds containing nitrogen and sulfur atoms that are predicted as active groups against antiplasmodial. This study aimed to synthesize two compounds derived from methyl eugenol, namely (1) isothiocyanates-based methyl eugenol and (2) thiosemicarbazide-based methyl eugenol. The synthesized compounds were characterized using FTIR, LCMS-MS, dissolution test, XRD, and SEM. The synthesized compounds were also tested in vitro for *Plasmodium falciparum* 3D7, molecular docking, and drug-likeness. Compound (1) was synthesized using methyl eugenol and thiocyanic acid at room temperature for 24 hours. The orange-coloured powder obtained contains dimer methyl eugenol isothiocyanate with a specific isothiocyanate wavenumber at 2055 cm^{-1} and molecular mass m/z 416. Compound (2) was synthesized using compound (1) and hydrazine for 10 hours. The specific wavenumber of (2) was identified at 1648 cm^{-1} (amine-free) and molecular mass of m/z 804. Compounds (1) and (2) have crystallite sizes of 5.38141 nm and 3.85276 nm, respectively. In vitro *Plasmodium falciparum* analysis resulted in IC_{50} of 0.34 µg/mL for (1) and 1.47 µg/mL for (2). Molecular docking analysis showed that (1) and (2) had binding energies of -6.0 kcal/mol and -1.2 kcal/mol. Compounds (1) and (2) had character deviations of drug-likeness. The drug formulation development is suggested to overcome the drug-likeness aspect, considering the in vitro antimalarial potentials in the two synthetic products.

Keywords: Isothiocyanate, Methyl eugenol, *Plasmodium falciparum*, Thiosemicarbazide.

Introduction

Malaria disease caused by pathogenic protozoa from the *Plasmodium falciparum* type is deadly because it can cause brain, lung, and kidney damage. This problem is becoming increasingly critical with drug and multidrug resistance, contributing to high morbidity and mortality rates.[1–3] Many medicinal plants such as *Moringa oleifera* leaves, *Citrullus colocynthis*, *Buxus hyrcana*, *Physalis alkekengi*, *Glycyrrhiza glabra*, *Ferula oopoda*, *Kigelia africana*, and *Nauclea latifolia* have been studied as an alternative to the antimalarial drug.[4–7] Essential oil-producing plants also attract attention because they contain major compounds that can be used as building blocks for drug synthesis.[8–10] One of the primary compounds in essential oil-producing plants is methyl eugenol. Methyl eugenol (ME) has been known as a compound with various bioactivities, including an active compound against Aedes aegypti larvae, anticonvulsants, and anesthetics.[11–17] Methyl eugenol can be obtained from the isolation of *Boesenbergia pulcherrima*, *Ocimum basilicum*, *Magnolia salicifolia*, *Lycium minutifolium*, and *Hedyosmum racemosum* (Ruiz & Pav.) G., *Brazilian red propolis*, *Pimenta pseudo caryophyllous,* and *Marrubium vulgare* plants.[13,18–24] Methyl eugenol can also be obtained through eugenol compound methylation. Many methyl eugenol conversions from eugenol have been reported.[25,26]

*Corresponding author. E mail: lucy.brawijaya@gmail.com
Tel: +62 82321885979

Citation: Arianie L, Supriatna MI, Kazal N, Widodo N, Warsito W, Iftitah ED. Synthesis, *In vitro*, and *In silico* Studies of Methyl Eugenol Derivatives for *Plasmodium falciparum* Inhibitor. Trop J Nat Prod Res. 2022; 6(9):

Official Journal of Natural Product Research Group, Faculty of Pharmacy, University of Benin, Benin City, Nigeria.

Eugenol is found abundantly in aromatic plants as an essential oil.[27–31] Eugenol is also potentially resourced from lignin degradation.[32,33] Methyl eugenol synthesized in the laboratory from natural eugenol extracts is often referred to as semisynthetic methyl eugenol. The molecular structure of methyl eugenol consists of three functional groups: the aromatic, methoxy and allyl terminal. The allyl-methyl eugenol is predicted to be convertible to methyl eugenol thiosemicarbazide. The synthesis goes through the intermediate formation of methyl eugenol isothiocyanate. There have been reports on producing some thiosemicarbazide compounds from isothiocyanate compounds.[34,35] Natural and synthetic isothiocyanates have bioactivities. For example, allyl isothiocyanate has antimicrobial properties, and benzyl isothiocyanate has been tested for herbal dental care.[36,37] Phenetyl isothiocyanate has anti-cytotoxic and antibacterial potentials.[38,39] In addition, propyl isothiocyanate compounds have also been observed to induce apoptosis in gastric cancer cells.[40] However, synthesis and analysis of methyl eugenol isothiocyanate for antimalarials were under-investigated and imperative to study. The selection of methyl eugenol thiosemicarbazide for the synthesis target compound in this research was because studies have reported that several thiosemicarbazides have various bioactivities. For example, Schiff base 4-ethy-1-(pyridin-2-yl)thiosemicarbazide (HEPTS) has been examined as an anti-tumor and thiosemicarbazide-chitosan for antibacterial.[41,42] A comparison of the inhibitory activities of noscapine derivatives showed that the noscapine thiosemicarbazide had better antiplasmodial activity and selectivity than the noscapine isothiocyanate.[43] Isothiocyanate and thiosemicarbazide compounds contain nitrogen and sulfur atoms. Compounds containing nitrogen and sulfur atoms play an essential role in many bioactivities.[34]

Preliminary research on methyl eugenol isothiocyanate by in silico approach has shown that methyl eugenol isothiocyanate is a potential *Plasmodium falciparum* inhibitor. It will have better properties if it has additional active groups.[4] Although the derivatization of methyl

 ISSN 2616-0684 (Print)
ISSN 2616-0692 (Electronic)

eugenol with thiocyanic acid and hydrazine tends to produce polymers, the potential of methyl eugenol derivative polymers for in vitro antimalarials is yet unidentified. To gather evidence on methyl eugenol derivative's potential against *Plasmodium falciparum*, the conversion of methyl eugenol to (1) methyl eugenol isothiocyanate and (2) methyl eugenol thiosemicarbazide, studies on the characterization product obtained, in vitro antimalarial assay and in silico analysis were conducted.

Materials and Methods

Materials

The materials of this study were methyl eugenol (99,0%), *dimethyl sulfoxide* (DMSO), potassium hydrogen sulfate, potassium thiocyanate, chloroform, ethyl acetate, diethyl ether, n-hexane, hydrazine monohydrate, methanol, ethanol, potassium bromide, aquadest, and TLC plate Silica gel 60 F_{254}. All chemicals used were pro-analysis grade. The methyl eugenol used was synthesized by PT Indesso. This methyl eugenol was synthesized from purified eugenol extracts derived from *Eugenia caryophyllata*. The clove flower bud and the methyl eugenol structure are illustrated in Figures 1a and 1b.

Synthesis and analysis of the compound (1)

Batista's (2019) and Silva's (1994) procedures were modified to synthesize isothiocyanate-based methyl eugenol (compound 1).[44,45] The orange-coloured powder obtained was dried from chloroform by using Nitrogen gas flow. The product was examined using Thin Layer Chromatography (TLC) using hexane-ethyl acetate (1:1, v/v) as the mobile phase. The product was also analyzed using dissolution test, Fourier Transform Infrared (FTIR), LCMS-MS (Liquid Chromatography Mass Spectrometry–Mass Spectrometry), SEM (Scanning electron microscope), XRD (X-Ray diffraction), and 3D7 *Plasmodium falciparum* malaria test.

Synthesis and analysis of the compound (2)

Thiosemicarbazide-based methyl eugenol (compound 2) was synthesized by using modified Yamaguchi's (2009) and Rodrigues (2018) methods.[46,47] Compound (1) was dissolved in 25 mL ethanol, to which hydrazine was added. The reaction occurred under the control of nitrogen gas flow, constant stirring, and a reaction temperature of 70°C. The yellow solid product was vacuum filtrated and weighed.

The influences of hydrazine monohydrate concentration (mmol) on the formation of compound (2) was observed at ratio of compound (1) to hydrazine at 0.4:0.4 (mmol), 0.4:0.5 (mmol), 0.4:0.6 (mmol), 0.4:0.7 (mmol), and 0.4:0.8 (mmol). The concentration of the compound that produces the highest mass of the product was set as the optimum condition. The effect of reaction time on the product (2) obtained was observed at 5, 6, 7.5, 9, and 10 hours into the experiment. The reaction time dependence on the product formation was analyzed using the optimum reactant ratio. The yellow-coloured powder obtained was tested using TLC analysis, dissolution test, FTIR, LCMS-MS, SEM, XRD, and 3D7 *Plasmodium falciparum* malaria test.

Crystallite size analysis

The crystal size of compounds (1) and (2) were measured with X-ray Diffractometer XPert MPD, with a Cu Kα radiation of 1.54 Å at 40 kV and 30 mA. The spectra were processed using Origin software to get β, the Bragg's angle (θ) and FWHM (full width of the diffraction peak measured at half maximum height). The crystal κ value was between 0.89 - 0.94. In this report, the κ value of 0.94 was used.[48–50] The observation of theta range was focused on 10° – 40°. The crystallite size (D) was measured by using the Scherrer equation:

$$D = \frac{\kappa \lambda}{\beta \cos \theta}$$

Antimalarial activity assay

The antimalarial assay was carried out using a modified Florence (2022) procedure.[51] Chloroquine-sensitive *Plasmodium falciparum* strain 3D7 was used. The sample was prepared by diluting a 10 mg sample in 1000 µL DMSO.

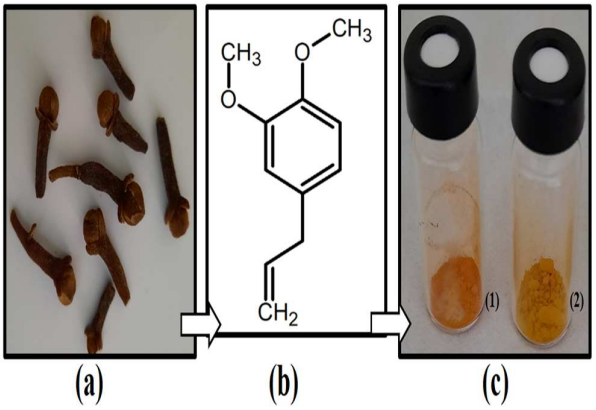

Figure 1: Clove flower bud (a); Methyl eugenol structure (b); The appearance of compounds (1) and (2) (c).

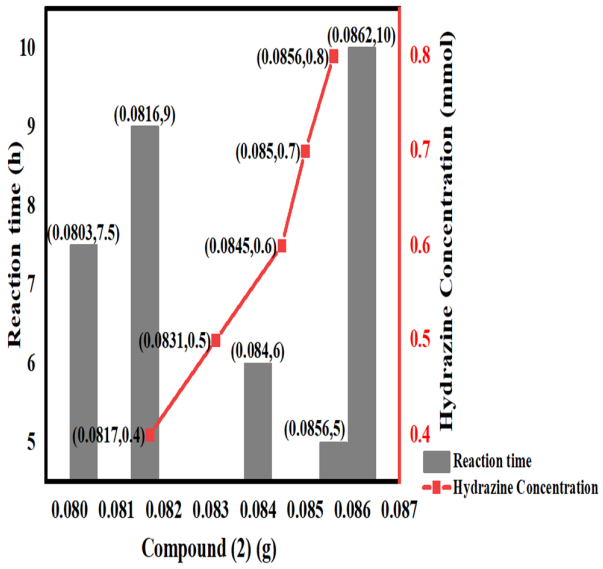

Figure 2: The compound (2) graph was obtained with the reagent concentration and reaction time variation.

Then, these concentrations were made: 1000, 100, 10, 1.0 and 0.1 µg/mL. The 50% inhibitory concentration (IC_{50}) was determined by probit analysis. D_0 is the growth of parasites at zero hours (%), Xt is the parasite's growth in the test solutions (%), and Xc is the growth of parasites in the negative control solution (%).

% Parasite's Growth = % parasitemia - D_0
% Inhibition = 100% - [(Xt - Xc) x 100%]

Molecular docking and drug-likeness analysis

A docking experiment revealed the binding modes of compounds (1) and (2) with the cysteine protease receptor. The receptor was downloaded from the protein data bank with PDB ID 1YVB. The receptor was optimized by removing the native ligand, water, and chain I. The structure of (1) and (2) was directly drawn using the Chemsketch program and well prepared as ligands (1) and (2) by Chimera. The molecular docking was run using PyRx.[52–54] The docking centers were set at 83.4002; -34.6003; -93.4099 for x, y, and z, respectively. The grid box dimensions were set at x = 14.9084; y = 18.3757; z = 14.6403. The docking result was analyzed and visualized using discovery studio visualizer. The drug-likeness was analyzed with SwissADME. This program was also used to analyze compounds' physicochemical and pharmacokinetic aspects.

 ISSN 2616-0684 (Print)
ISSN 2616-0692 (Electronic)

Instrumentation and sample preparation

The functional group of compounds was investigated with the potassium bromide pellet and spectrophotometer Fourier Transform Infrared Shimadzu at 500–4000 cm^{-1} wavenumber observation. LCMS/MS analysis was carried out using triple quadrupole 8060 Shimadzu, column Cosmosil 5C18-MS-II (4.6 i.d. × 150 mm; Nacalaitesque). Gradient elution consisted of eluent A (water in 0.1% formic acid) and eluent B (acetonitrile). The eluent at 0 minute (min) was 5% B; 0–3 min: 5% B–85% B; 3–4 min: 85% B; 4–6 min: 90% B; and 6–10 min: 100 % B. The flow rate was set to 0.3 mL/minute, and the column temperature was maintained at 25 °C. MS/MS detection was equipped with an electrospray ionization interface (ESI) operating in the positive and negative ion modes. The preparation sample of LCMS-MS was done by diluting the sample in 1.5 mL methanol, sonicating solution for 1 minute, and filtering the supernatant with PTFE 0.22 µm. About 20 µL of samples were injected into the chromatographic instrument. The FEI inspect S50 instrument with 5000x magnification was used to observe the morphology of the compound surface.

Results and Discussion

Synthesis and analysis of the compounds (1) and (2)

The reaction mechanism of isothiocyanate-based methyl eugenol was under Markovnikov's rule in which thiocyanate compounds were also formed.[55] Compound (1) was derived predictively from methyl eugenol and isothiocyanate methyl eugenol polymerization. The polymerization mechanism predictively occurred because the double bond in the methyl eugenol tail was activated under acidic conditions, then charged positive and negative partially. One hydrogen cation of thiocyanic acid was bonded to hydrogen-rich carbon. Another allyl-methyl eugenol further attacked that positive charge to form polymeric chains. The synthesized product was orange-colored powder. (See the left part of Figure 1c.) This product would be used as the precursor to form compound (2). Methyl eugenol isothiocyanate has a synthetic accessibility score of 2.51. The compound (1) was estimated to be synthesized easily on a laboratory scale.[4]

Compound (2) was synthesized using compound (1) and hydrazine monohydrate with various hydrazine concentration ratios. Precursor to hydrazine ratios used were at 0.4:0.4 (mmol), 0.4:0.5 (mmol), 0.4:0.6 (mmol), 0.4:0.7 (mmol), 0.4:0.8 (mmol), and resulted in the best ratio at a 0.4:0.8 (mmol) with maximum product gain (0.0862 g). The reaction time dependence to compound (2) formation was observed for 10 hours. The synthesis reaction time was positively correlated with compound (2) formation (Figure 2). Thiosemicarbazide-based methyl eugenol, laid out on the right side, was illustrated in Figure 1c. The concentration ratio and the time reaction affected compound (2) formation.

Analysis of functional groups

The infrared spectra of compounds (1) and (2) were compared directly with the infrared spectrum of methyl eugenol. In Figure 3a, the methyl eugenol infrared and compound (1) range from 500 cm^{-1} to 2500 cm^{-1}. The research found there were significant changes in the spectra (1), i.e. the appearance of an isothiocyanate-specific wavenumber (around 2050 cm^{-1}) and the disappearance of the allyl-methyl eugenol peak (about 900 cm^{-1}) in compound (1) spectrum.[56,57] It predictively confirms that an addition reaction of the double bond allyl-methyl eugenol into a single bond has occurred. A comparison of the infrared spectra of compounds (1) and (2) shows that thiosemicarbazide-based methyl eugenol has been formed (Figure 3b). It was identified by the loss of the isothiocyanate peak (2050 cm^{-1}), and a new peak at 3200 cm^{-1}–3500 cm^{-1} for the primary amine was shown. Several wavenumbers strongly supported that compound (2) was formed, i.e. the carbon-sulfur bond (620 cm^{-1}), carbon-nitrogen bond (1120 cm^{-1}), and the single bond between nitrogen and hydrogen at 1600 cm^{-1}.

Molecule ion analysis

Molecule ion analysis of the synthesis product was carried out using LCMS-MS. The results showed predictively that m/z 416 was a dimer of methyl eugenol isothiocyanate and m/z 803 was a tetramer of methyl eugenol thiosemicarbazide. MS data confirmed the dimers and tetramers forming isothiocyanate and thiosemicarbazide in methyl eugenol. The phenomenon of polymerization of allyl groups in eugenol has been reported. The activity of allyl groups in eugenol was observed in concentrated sulfuric acid at room temperature to produce polyeugenol.[58] Polymerization was also formed in the synthesis of limonene isothiocyanate derived from limonene and thiocyanic acid sources.[44] Identical to methyl eugenol, limonene has a terminal double bond that an addition reaction mechanism can occur to form the isothiocyanate bond. The polymerization of methyl eugenol derivatives using allyl-methyl eugenol groups with a Rhodium catalyst was carried out to produce poly (N-propargyl carbamate). This polymerization occurred via the allyl- methyl eugenol transformation into a 2-hydroxy group.[59] The polymerization of eugenol and methyl eugenol was also carried out by using Rh (Rhodium), Mo (Molybdenum), and Wolfram (W) catalysts. Its methyl eugenol polymerization is possible through the methoxy-eugenol and methoxy-methyl eugenol or allyl groups.[60]

Dissolution test

The solubility of compounds (1) and (2) was tested using several solvents by inserting 2 mg of the sample in a test tube and then adding 2 milliliters of the test solvent. The test results showed that all compounds were well dissolved in DMSO but poorly in water (Table 1). The solubility of a drug is related to its bioavailability. Drug candidates should be able to dissolve in water less than 1 µg/mL to meet the bioavailability standards.[61]

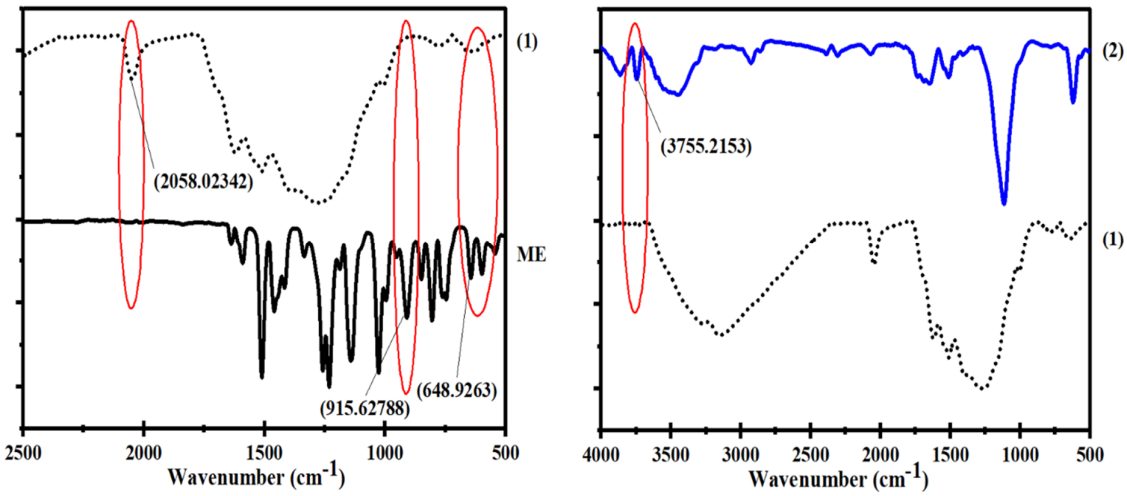

Figure 3: The infrared spectra of methyl eugenol and product obtained.

 ISSN 2616-0684 (Print)
ISSN 2616-0692 (Electronic)

Table 1: Dissolution test of compounds (1) and (2)

Compound:	Solvent:						
	Diethyl ether	Ethyl acetate	Methanol	n-Hexane	Ethanol	DMSO	Aquadest
1	+	-	-	+	+	+++	+
2	++	+	-	+	+	+++	+

* - not dissolved, + slightly dissolved, ++ partially dissolved, +++ completely dissolved.

Table 2: Drug-likeness of compounds (1), (2), and chloroquine

Compound	Lipinski Rule*					Veber Rule**	
	MW	HBA	HBD	LogP	Molar Rf	RB	TPSA
1	415.55	5	0	4.48	119.87	11	81.37
2	802.05	9	3	6.12	230.59	25	156.01
Chloroquine	319.88	2	1	3.95	97.41	8	28.16

*Lipinski rule: MW: Molecular Weight ≤500g/mol, HBA: Hydrogen Bond Acceptor ≤10, HBD: Hydrogen Bond Donor ≤5, LogP ≤5, Molar Refractivity 40-130.
**Veber rule: RB: Rotatable Bond ≤10, TPSA: Topological Polar Surface Area (Å) ≤140.

Morphological surface analysis
SEM experiment was used for morphological surface analysis. SEM imaging of the synthesized compound was shown in Figure 5. The two compounds had different surface displays; compound (1) showed more agglomeration than (2).

Crystallite size of compounds (1) and (2)
From the MS data, solubility test, and SEM image, it was known that compounds (1) and (2) had high molecular weight, bulk, and low solubility in water. Drug candidates with poor solubility in water will be difficult to digest. These compounds are classified as category 2 or 4 in the biopharmaceutical classification system (BCS).[61] This unacceptable drug-likeness character can be overcome using drug formulation techniques by considering the Critical Quality Attributes (CQAs) and nanosuspension drug candidate parameters, including particle size and crystallinity.[62] Therefore, the crystal size (D) of these two powders was measured by the Scherrer equation, showing D = 5.38141 nm and D = 3.85276 nm for compounds (1) and (2), respectively. The crystallinity degree was also observed since it is one of the keys to predicting the solubility of drugs in water and octanol.[63] A comparison between the X-ray diffraction peaks of compounds (1) and (2) was presented in Figure 6. The observation of the spectra suggested that qualitatively compound (1) was more crystalline than compound (2).

Antimalarial activity of compounds (1) and (2)
In vitro assay is an essential aspect of drug candidates. Drug compounds with low solubility and permeability can be improved if they have highly active in vitro values. The in vitro analysis of compounds (1) and (2) using *Plasmodium falciparum* was depicted in Figure 7. The graph presents the average value of inhibition and growth of parasites resulting from the concentration variations of the compounds. Statistical analysis was conducted to determine the IC_{50}. The in vitro antimalarial test identified compounds (1) and (2) had IC_{50} of 0.34 µg/mL and 1.47 µg/mL, respectively. Figure 7 indicates that the higher the concentration of the drug candidate, the higher the inhibition against the growth of *Plasmodium falciparum* parasites. This study also indicates that the smaller the compound concentration, the higher the growth (%) of *Plasmodium falciparum*. The compounds (1) and (2) were more potent against the parasite than chloroquine as an antimalarial reference by IC_{50} value of 4.81 µg/mL.[64]

Molecular docking and drug-likeness of compounds (1) and (2)
Molecular docking analysis was carried out to determine the interaction of the ligand with the *Plasmodium falciparum* malaria receptor. This analysis requires a receptor with active sites and a drug candidate as a ligand. The *Plasmodium falciparum* receptor used in this study was 1YVB chain A. Receptor is a macromolecule (lipoprotein or nucleic acid) in the cell membrane or nucleus. Receptors have specific atoms or functional groups that act as active sites and will interact with drug compounds to produce specific biological responses.[65–67] Active sites in 1YVB are Cysteine and Histidine.[68] The complex interaction of receptor and ligand was identified in Figure 8. It can be seen that ligand (1) had a pi-amide bond and a pi-donor hydrogen bond between histidine-159 and the aromatic-methyl eugenol.

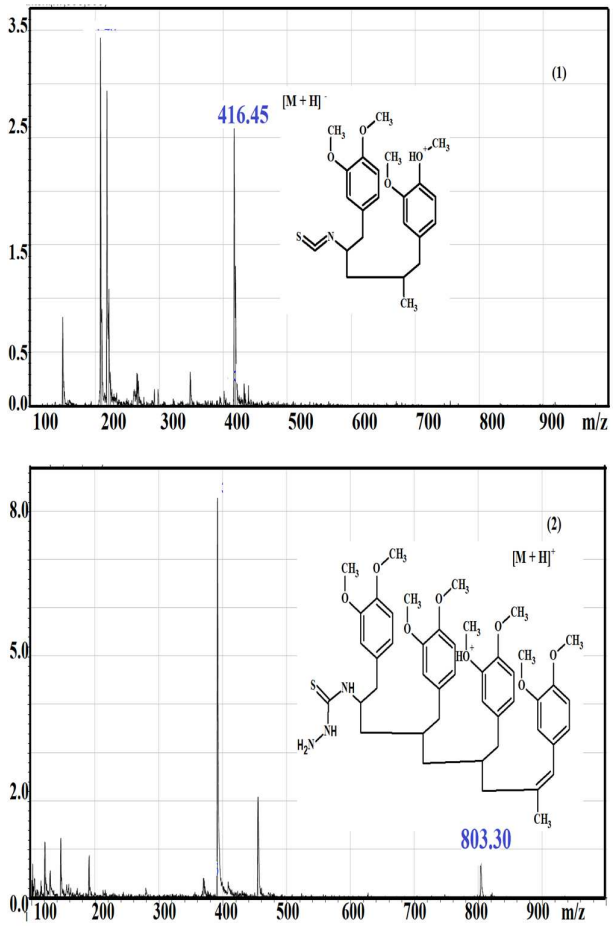

Figure 4: The spectra and structure prediction of compounds (1) and (2).

The second receptor active site, cysteine-25, interacted with another aromatic-methyl eugenol via a pi-alkyl bond. At the same time, ligand (2) did not have hydrogen bonding interactions with the receptor's active site. It predictively affected to IC_{50} value. Ligand (1) interacted with the receptor and had better IC_{50} values than (2).
For comparison, molecular docking was also run for chloroquine (a standard malaria drug). The analysis showed that ligand (1) had the best affinities (ΔG) values at -6.0 kcal/mol. The value of ligand (1) was lower than that of chloroquine (-5.3 kcal/mol) and ligand (2) (-1.2 kcal/mol). These affinity energies indicate that the complex ligand (1) and 1YVB chain A are the most stable.[69] All the affinities were obtained at an RMSD (Root Mean Standard Deviation) of 0.0.
Biological activity resulting from ligand-receptor interactions that contribute to a disease's healing process was called an agonist, and the opposite was called an antagonist. Meanwhile, the relationship between receptors and ligands between agonists and antagonists was known as partial antagonists.[65–67] Based on the IC_{50} values of compounds (1) and (2), it can be assumed that these two compounds are agonists.

Physicochemical, pharmacokinetic and drug-likeness
SwissADME was used to assess the physicochemical and pharmacokinetic characteristics of the drug candidates. The drug-likeness of compounds (1) and (2) was presented in Table 2 which compares by chloroquine character.[4,70] The physicochemical of compounds (1) and (2) were analyzed by radar bioavailability. This model represents physicochemical characteristics such as lipophilicity (LIPO), molecule size (SIZE), polarity (POLAR), solubility (INSOLU), saturation (INSATU), and flexibility (FLEX).
The requirements for the lipophilicity range (XLog P3) that must be met are between -0.7 and +1.5. The molecular size (MW) must be between 150 and 500 g/mol. The required polarity should be 20 $Å^2$ to 130 $Å^2$, the solubility range (LogS ESOL) between 0.0 to 6.0, and saturation (Carbon fraction in the sp^3 hybridization) at 0.25 to 1.0. The last requirement in the bioavailability radar is that a drug candidate must have a maximum value of 9 for molecular flexibility. This flexibility correlates with rotatable bonds of ligands that interact with receptors.[71,72] The tested molecule qualified against the drug-likeness rule is symbolized with a bold blue line within the dotted red lines of the bioavailability radar. The physicochemical evaluation of compounds (1) and (2) was presented in Figure 9. Compound (1) had two characters (flexibility and lipophilicity) outside the dotted red line, while compound (2) had four deviations: flexibility, lipophilicity, molecule size, and solubility. Compounds (1) and (2) showed low flexibility and lipophilicity levels, indicated by lines outside the bioavailability radar limit. Low flexibility will affect the ability of the drug to interact with target receptors. The lipophilicity section affects the absorption ability of drug candidates in fat. The pharmacokinetic characteristics of compounds (1) and (2) were evaluated using the Boiled-egg model. This model represents the absorbability of candidate drugs in the digestive tract or gastrointestinal tract (Gastrointestinal absorption = GIA). This model also describes the permeability of compounds in the blood-brain barrier system (blood-brain barriers =BBB). In the boiled-egg model, the GIA area is represented by the egg white area and the BBB area in the yolk section. Compound (1) was predicted to be well absorbed in the gastrointestinal tract. However, the compound (2) result could not be interpreted because the compound symbol (2) position was outside the boiled egg model. Chloroquine, a standard antimalarial drug, was tested for comparison (Figure 10). This research revealed compound (1) as a promising *Plasmodium falciparum* antimalarial drug candidate. This preliminary research merits further investigation for structure elucidation. The molecular size reduction might overcome compounds' physicochemical and pharmacokinetic problems of (1) and (2). This includes considering new synthetic pathways to produce methyl eugenol isothiocyanate and methyl eugenol thiosemicarbazide without polymerization. As previously discussed, the formulation of the drug compounds may overcome the physicochemical and pharmacokinetic deviations. One method of drug formulation is through drug nanosuspension, which accounts for the drug's crystal size. Based on the IC_{50} values of the two synthetic products, it is necessary to consider controlling the physicochemical/pharmacokinetic aspects and the drug-likeness.

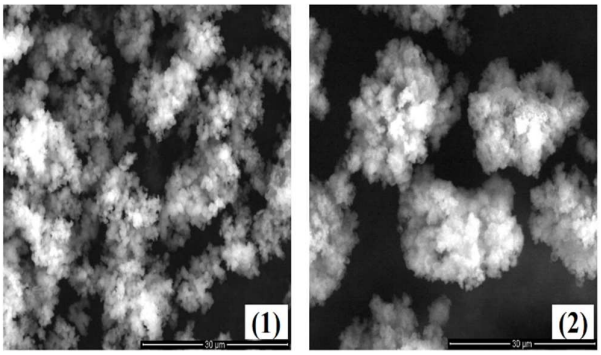

Figure 5: The appearance on the surface of compounds (1) and (2).

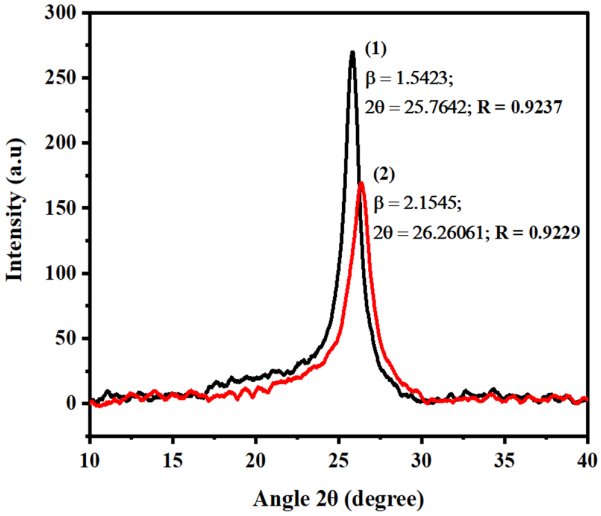

Figure 6: The X-Ray diffraction spectra of compound (1) and compound (2).

To develop isothiocyanate-based methyl eugenol derivate as a drug candidate, nanosuspension and encapsulation must be considered because these methyl eugenol derivatives are unstable compounds.
Nowadays, manufacturing drugs in nanosuspension form have become a trend. The advantages of nanosuspension drug formulations are high drug loading, minimum side effects of excipients, low production costs, and easy scaling up.[62]

Conclusion

Methyl eugenol derivates that contain nitrogen and sulfur atoms, namely isothiocyanate-based methyl eugenol and thiosemicarbazide-based methyl eugenol, were synthesized in this study. Analysis using infrared and mass spectroscopy showed that compound (1) was predicted as a dimer of methyl eugenol isothiocyanate and compound (2) was a tetramer of methyl eugenol thiosemicarbazide. These two synthetic compounds are poorly soluble in water and highly soluble in DMSO. The surface morphology and crystal size of compounds (1) and (2) showed that these compounds had different surface morphology. The crystals (1) and (2) were 5.38141 nm and 3.85276 nm in size, respectively. Compounds (1) and (2) were highly active against *Plasmodium falciparum* 3D7.
Observations using molecular docking demonstrated that compound-receptor complex (1) had better binding energy than compound (2) or chloroquine as a standard antimalarial drug. However, physicochemical and pharmacokinetic testing showed that the two synthesized compounds had deviations in drug-likeness characteristics.

ISSN 2616-0684 (Print)
ISSN 2616-0692 (Electronic)

Conflict of Interest

The authors declare no conflict of interest.

Authors' Declaration

The authors hereby declare that the work presented in this article is original and that any liability for claims relating to the content of this article will be borne by them.

Acknowledgements

This project was partially funded through the Hibah Guru Besar 2020-2021. All authors would like to gratefully acknowledge the Ministry of Research, Technology, and Higher Education of the Republic of Indonesia. Great appreciation and gratitude are also sent to Institut Atsiri and the Faculty of Science - Brawijaya University for providing research facilities. This article is part of the doctoral study.

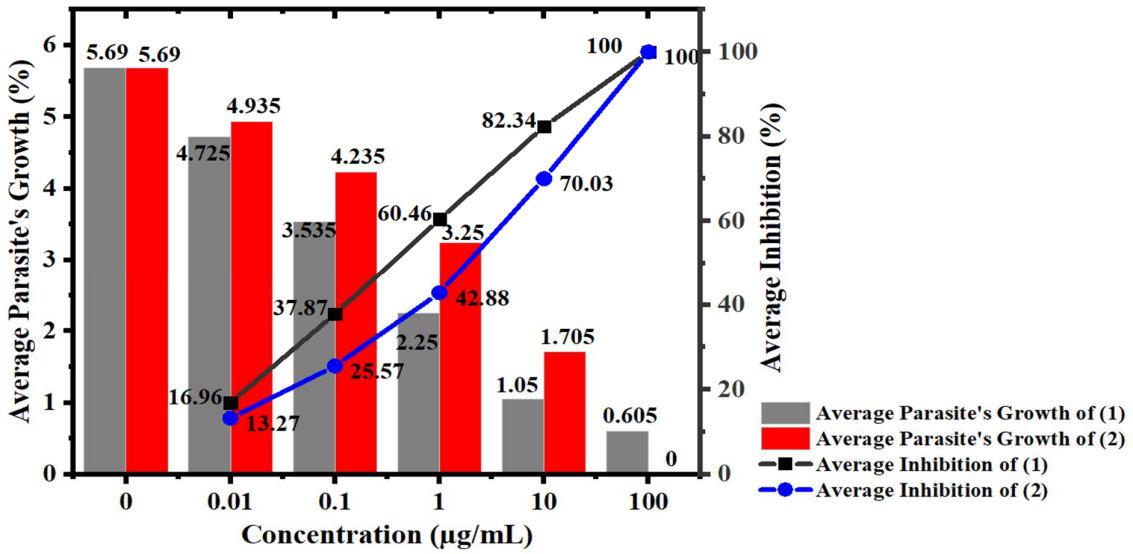

Figure 7: *In vitro* anti-malaria analysis of compound (1) and compound (2).

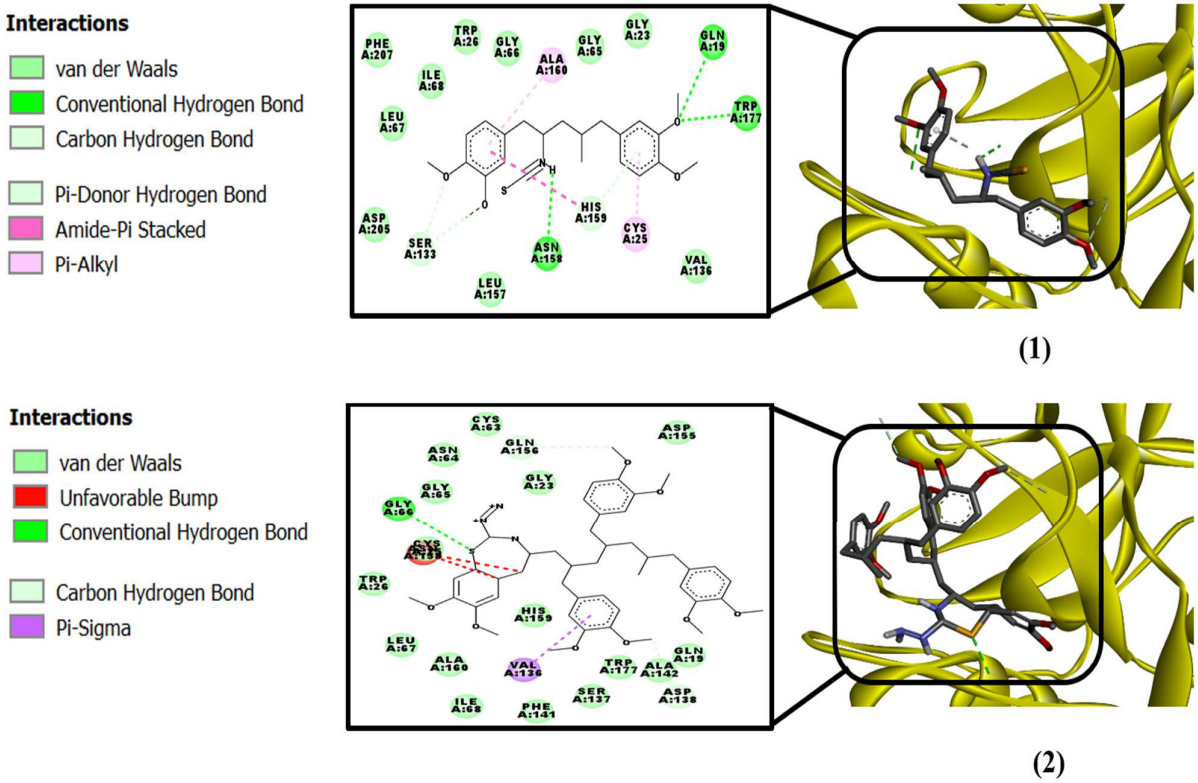

Figure 8: The interaction of 1YVB chain A with ligands (1) and (2).

 ISSN 2616-0684 (Print)
ISSN 2616-0692 (Electronic)

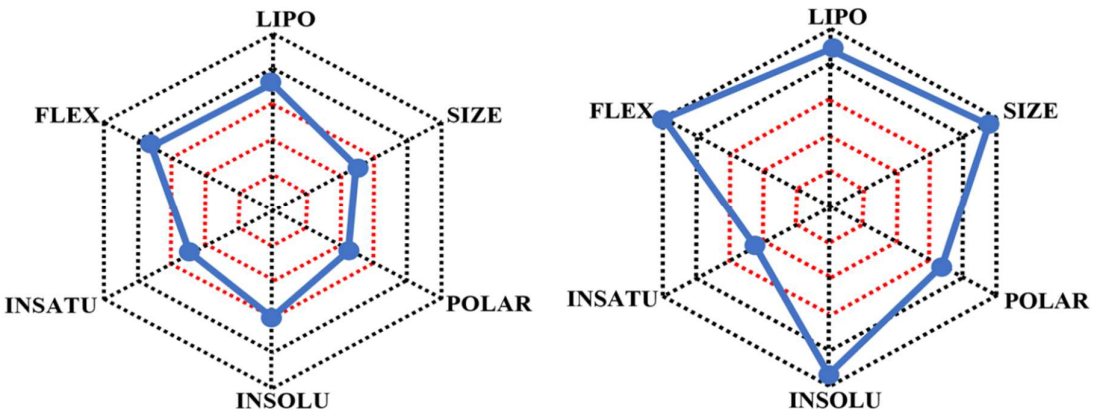

Figure 9: The bioavailability radar of compounds (1) and (2).

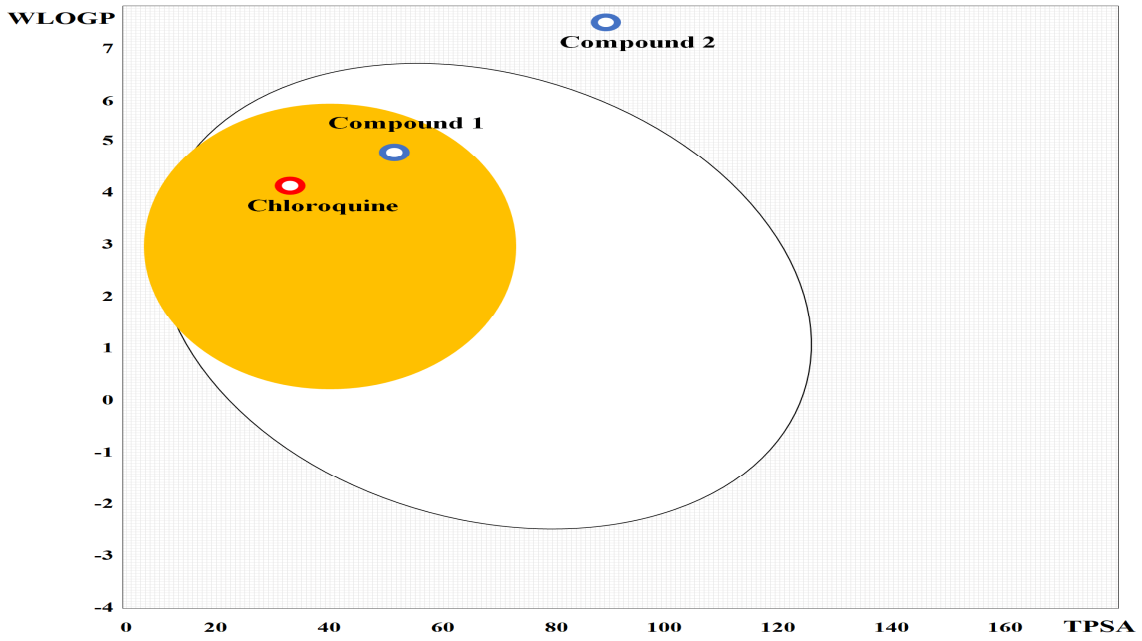

Figure 10: The boiled-egg model of compounds (1), (2), and chloroquine.

References

1. Odoh UE, Uzor PF, Eze CL, Akunne TC, Onyegbulam CM, Osadebe PO. Medicinal plants used by the people of Nsukka Local Government Area, south-eastern Nigeria for the treatment of malaria: An ethnobotanical survey. J Ethnopharmacol. 2018; 218(1): 1–15.
2. Barabadi H, Alizadeh Z, Rahimi MT, Barac A, Maraolo AE, Robertson LJ, Masjedi A, Shahrivar F, Ahmadpour E. Nanobiotechnology as an emerging approach to combat malaria: A systematic review. Nanomedicine: NBM. 2019; 18(4): 221–233.
3. Maier AG, Matuschewski K, Zhang M, Rug M. *Plasmodium falciparum*. Trends Parasitol. 2019; 35(6): 481–482.
4. Arianie L, Widodo, Iftitah ED, Warsito. Natural Isothiocyanate Anti-Malaria: Molecular Docking, Physicochemical, ADME, Toxicity and Synthetic Accessibility Study of Eugenol and Cinnamaldehyde. Int J Appl Pharm. 2021; 13(6): 82–88.
5. Leone A, Spada A, Battezzati A, Schiraldi A, Aristil J, Bertoli S. Cultivation, Genetic, Ethnopharmacology, Phytochemistry and Pharmacology of *Moringa oleifera* Leaves: An Overview. Int J Mol Sci. 2015; 16(12): 12791–12835.
6. Mehravaran A, Mirahmadi H, Mohamadi L, Dahmardeh H. Traditional herbal treatment for *Plasmodium falciparum*: A systematic review on traditional plants to treat malaria in Iran. Int J Psychosoc Rehabilitation. 2020; 24(5): 7469–7481.
7. Ikem CJ, Oli AN, Ofori-Attah E, Aning A, Regina A-O, Esimone CO. Screening of Five Herbal Formulations Sold in South-East Nigeria for Their Phytochemical Properties, *in Vitro* Antioxidant, Antiplasmodial and Cytotoxic Activities. Trop J Nat Prod Res. 2022; 6(1): 150–155.
8. Bekele D. Review on Insecticidal and Repellent Activity of Plant Products for Malaria Mosquito Control. Biomed Res Rev. 2018; 2(2): 1–7.
9. Luo D-Y, Yan Z-T, Che L-R, Zhu JJ, Chen B. Repellency and insecticidal activity of seven Mugwort (*Artemisia argyi*) essential oils against the malaria vector anopheles sinensis. Sci Rep. 2022; 12(1): 5337.
10. Pontes KAO, Silva LS, Santos EC, Pinheiro AS, Teixeira DE, Peruchetti DB, Silva-Aguiar RP, Wendt CHC, Miranda KR,

Coelho-de-Souza AN, Leal-Cardoso JH, Caruso-Neves C, Pinheiro AAS. Eugenol Disrupts *Plasmodium falciparum* Intracellular Development During the Erythrocytic Cycle and Protects Against Cerebral Malaria. Biochim Biophys Acta - Gen Subj. 2021; 1865(3): 129813.

11. Sarma R, Adhikari K, Mahanta S, Khanikor B. Combinations of Plant Essential Oil Based Terpene Compounds as Larvicidal and Adulticidal Agent against *Aedes aegypti* (Diptera: Culicidae). Sci Rep. 2019; 9(1): 9471.
12. Voris DG da R, dos Santos Dias L, Alencar Lima J, dos Santos Cople Lima K, Pereira Lima JB, dos Santos Lima AL. Evaluation of Larvicidal, Adulticidal, and Anticholinesterase Activities of Essential Oils of *Illicium verum* Hook. F., *Pimenta dioica* (l.) Merr., and *Myristica Fragrans* Houtt. Against Zika Virus Vectors. Environ Sci Pollut Res. 2018; 25(23): 22541–22551.
13. Kelm MA, Nair MG, Schutzki RA. Mosquitocidal Compounds from *Magnolia salicifolia*. Int J Pharmacogn (Lisse, Neth). 1997; 35(2): 84–90.
14. Ronal A, Astuti FN, Pratiwi L, Prihastari L. Preliminary Study on the Potential of Topical Anaesthesia from Betel Leaf and Clove Leaf Extract. Padjadjaran J Dent. 2021; 33(3): 250–257.
15. Khumpirapang N, Pikulkaew S, Anuchapreeda S, Okonogi S. Anesthetic activity of plant essential oils on *Cyprinus carpio* (koi carp). Drug Discoveries Ther. 2018; 12(1): 21–30.
16. Wang Z-J, Tabakoff B, Levinson SR, Heinbockel T. Inhibition of Nav1.7 Channels by Methyl Eugenol as a Mechanism Underlying Its Antinociceptive and Anesthetic Actions. Acta Pharmacol Sin. 2015; 36(7): 791–799.
17. Aydın B, Barbas LAL. Sedative and anesthetic properties of essential oils and their active compounds in fish: A review. Aquaculture. 2020; 520(1): 734999.
18. Vural N. Chemometrics Data Analysis and Controversial Carcinogenic Effect of *Ocimum basilicum* L. Rich in Methyl Eugenol. Food Measure. 2021; 15(5): 4825–4837.
19. Park C, Kim H, Lee DW, Kim J, Choi Y. Identification of Antifungal Constituents of Essential Oils Extracted from *Boesenbergia pulcherrima* Against Fusarium Wilt (*Fusarium oxysporum*). Appl Biol Chem. 2020; 63(34): 1–8.
20. Rodriguez S, Pertino MW, Arcos C, Reichert L, Echeverria J, Simirgiotis M, Borquez J, Cornejo A, Areche C, Sepulveda B. Isolation, Gastroprotective Effects and Untargeted Metabolomics Analysis of *Lycium minutifolium* J. remy (solanaceae). Foods. 2020; 9(565): 1–12.
21. Valarezo E, Morocho V, Cartuche L, Chamba-Granda F, Correa-Conza M, Jaramillo-Fierro X, Meneses MA. Variability of the Chemical Composition and Bioactivity Between the Essential Oils Isolated from Male and Female Specimens of *Hedyosmum racemosum* (ruiz & Pav.) G. Don. Molecules. 2021; 26(4613): 1–14.
22. Sena-Lopes Â, Bezerra FSB, das Neves RN, de Pinho RB, Silva MT de O, Savegnago L, Collares T, Seixas F, Begnini K, Henriques JAP, Ely MR, Rufatto LC, Moura S, Barcellos T, Padilha F, Dellagostin O, Borsuk S. Chemical Composition, Immunostimulatory, Cytotoxic and Antiparasitic Activities of the Essential Oil from Brazilian Red Propolis. Chang I-F (ed.). PLoS ONE. 2018; 13(2): e0191797.
23. Niculau E, Ribeiro L, Ansante T, Fernandes J, Forim M, Vieira P, Vendramim J, da Silva M. Isolation of Chavibetol and Methyleugenol from Essential Oil of *Pimenta pseudocaryophyllus* by High Performance Liquid Chromatography. Molecules. 2018; 23(11): 2909.
24. Zatla AT, Mami I, Dib MEA, Sifi MEA. Efficacy of Essential Oil and Hydrosol Extract of *Marrubium vulgare* on Fungi Responsible for Apples Rot. Anti-Infect Agents. 2020; 18(3): 285–293.
25. Rahim EA, Sanda F. Synthesis and functionality of eugenol-based polyacetylenes. J Phys: Conf Ser. 2019; 1242(1): 012003.
26. Agustian E, Tursiloadi S, Sulaswatty A, Rinaldi N, Sudiyarmanto. One-Pot Conversion and Separation of Methyl Eugenol by Vacuum Fractionation. IOP Conf Ser: Mater Sci Eng. 2019; 494(012056): 1–7.
27. Kshirsagar P, Pawar D, Mourya P, Kamble O, Patil A. Isolation and Extraction of Eugenol from Cloves - a Review. World J Pharm Res. 2018; 7(5): 421–427.
28. Crouse BJ, Vernon EL, Hubbard BA, Kim S, Box MC, Gallardo-Williams MT. Microwave Extraction of Eugenol from Cloves: A Greener Undergraduate Experiment for the Organic Chemistry Lab. World J Chem Educ. 2019; 7(1): 21–25.
29. Bao H, Xu Y, Wang Y, Zhang T, Wang E, Huang X, Chen C, Liu F. Optimization of Extraction Process of Methyl Eugenol and Asarinin in Asarum with Deep Eutectic Solvent Based on the Response Surface Methodology. Mitu L (ed.). J Chem. 2021; 2021(2069986): 1–11.
30. Umaru IJ, Umaru KI, Umaru HA. Phytochemical Screening, Isolation, Characterization of Bioactive and Biological Activity of Bungkang, (*Syzygium polyanthum*) Root-Bark Essential Oil. KJFHC. 2020; 6(3): 5–21.
31. Frohlich PC, Santos KA, Palú F, Cardozo-Filho L, da Silva C, da Silva EA. Evaluation of the Effects of Temperature and Pressure on the Extraction of Eugenol from Clove (*Syzygium aromaticum*) Leaves Using Supercritical Co2. J Supercrit Fluids. 2019; 143(1): 313–320.
32. Sun Z, Fridrich B, de Santi A, Elangovan S, Barta K. Bright Side of Lignin Depolymerization: Toward New Platform Chemicals. Chem Rev. 2018; 118(2): 614–678.
33. Pedroza-Solis CD, Rivera De la Rosa J, Lucio-Ortiz CJ, De Haro Del Río DA, González-Casamachin DA, Hernández García TC, Flores Escamilla GA, Carrillo-Pedraza ES, Santos López IA, Bustos Martínez D, García-Gutiérrez DI, Sandoval Rangel L. Thermocatalytic degradation of lignin monomer coniferyl aldehyde by aluminum–boron oxide catalysts. Comptes Rendus Chimie. 2021; 24(S1): 101–117.
34. Acharya PT, Bhavsar ZA, Jethava DJ, Patel DB, Patel HD. A Review on Development of Bio-Active Thiosemicarbazide Derivatives: Recent Advances. J Mol Struct. 2021; 1226(Part A): 129268.
35. Dziduch K, Kołodziej P, Paneth A, Bogucka-Kocka A, Wujec M. Synthesis and Anthelmintic Activity of New Thiosemicarbazide Derivatives—A Preliminary Study. Molecules. 2020; 25(12): 2770.
36. Takahashi H, Nakamura A, Fujino N, Sawaguchi Y, Sato M, Kuda T, Kimura B. Evaluation of the Antibacterial Activity of Allyl Isothiocyanate, Clove Oil, Eugenol and Carvacrol Against Spoilage Lactic Acid Bacteria. LWT--Food Sci Technol. 2021; 145(12): 111263.
37. Abdel-Kader MS, Khamis EH, Foudah AI, Alqarni MH. GC Quantitative Analysis of Benzyl Isothiocyanate in *Salvadora persica* Roots Extract and Dental Care Herbal Products. Saudi Pharm J. 2018; 26(4): 462–466.
38. Dayalan Naidu S, Suzuki T, Yamamoto M, Fahey JW, Dinkova-Kostova AT. Phenethyl Isothiocyanate, a Dual Activator of Transcription Factors NRF2 and HSF1. Mol Nutr Food Res. 2018; 62(18): 1700908.
39. Nowicki D, Maciąg-Dorszyńska M, Bogucka K, Szalewska-Pałasz A, Herman-Antosiewicz A. Various Modes of Action of Dietary Phytochemicals, Sulforaphane and Phenethyl Isothiocyanate, on Pathogenic Bacteria. Sci Rep. 2019; 9(1): 13677.
40. Huang L, Cai C, Dang W, Lu J, Hu G, Gu J. Propyl Isothiocyanate Induces Apoptosis in Gastric Cancer Cells by Oxidative Stress Via Glutathione Depletion. Oncol Lett. 2019; 18(9): 5490–5498.
41. Aboseada HA, Hassanien MM, El-Sayed IH, Saad EA. Schiff Base 4-Ethyl-1-(pyridin-2-Yl) Thiosemicarbazide up-Regulates the Antioxidant Status and Inhibits the Progression of Ehrlich Solid Tumor in Mice. Biochem Biophys Res Commun. 2021; 573(40): 42–47.
42. Ahmad M, Ahmed S, Swami BL, Ikram S. Preparation and Characterization of Antibacterial Thiosemicarbazide Chitosan

as Efficient Cu(ii) Adsorbent. Carbohydr Polym. 2015; 132(18): 164–172.
43. Harikandei KB, Salehi P, Ebrahimi SN, Bararjanian M, Kaiser M, Al-Harrasi A. Synthesis, in-Vitro Antiprotozoal Activity and Molecular Docking Study of Isothiocyanate Derivatives. Bioorg Med Chem. 2020; 28(1): 115185.
44. Batista SA, Vandresen F, Falzirolli H, Britta E, de Oliveira DN, Catharino RR, Gonçalves MA, Ramalho TC, La Porta FA, Nakamura CV, da Silva CC. Synthesis and Comparison of Antileishmanial and Cytotoxic Activities of S-(−)-Limonene Benzaldehyde Thiosemicarbazones with Their R-(+)-Analogues. J Mol Struct. 2019; 1179(5): 252–262.
45. da Silva CC, Almagro V, Zukerman-Schpector J, Castellano EE, Marsaioli AJ. An Easy Route to (-)-10(R)-Isothiocyanoaromadendrane and (-)-10(S)-Isothiocyanoalloaromadendrane. J Org Chem. 1994; 59(10): 2880–2881.
46. Yamaguchi MU, Barbosa da Silva AP, Ueda-Nakamura T, Dias Filho BP, Conceição da Silva C, Nakamura CV. Effects of a Thiosemicarbazide Camphene Derivative on *Trichophyton Mentagrophytes*. Molecules. 2009; 14(5): 1796–1807.
47. Rodrigues BDS, de Ávila RI, Benfica PL, Bringel LP, de Oliveira CMA, Vandresen F, da Silva CC, Valadares MC. 4-Fluorobenzaldehyde limonene-based thiosemicarbazone induces apoptosis in PC-3 human prostate cancer cells. Life Sci. 2018; 203(12): 141–149.
48. Ilyas S, Heryanto, Abdullah B, Tahir D. X-ray diffraction analysis of nanocomposite Fe 3 O 4 /activated carbon by Williamson–Hall and size-strain plot methods. Nano-Struct Nano-Objects. 2019; 20(4): 100396.
49. Oluyamo SS, Adekoya MA. Characterization of cellulose nanoparticles for materials device applications and development. Materials Today: Proceedings. 2021; 38(Part 2): 595–598.
50. Jakubek ZJ, Chen M, Couillard M, Leng T, Liu L, Zou S, Baxa U, Clogston JD, Hamad WY, Johnston LJ. Characterization challenges for a cellulose nanocrystal reference material: dispersion and particle size distributions. J Nanopart Res. 2018; 20(98): 1–16.
51. Florence CC, Nonye NE, Josephine E-OO. *In vitro* antiplasmodial and *in vivo* toxicity potential of *Mentha piperita* and *Ocimum gratissimum* essential oils and their synergistic effect with conventional antimalarial drugs against *Plasmodium falciparum*. Int J Mosq Res. 2022; 9(1): 114–122.
52. Dallakyan S, Olson AJ. Small-Molecule Library Screening by Docking with Pyrx. In: Hempel JE, Williams CH, Hong CC (eds.). Chemical Biology. New York, NY: Springer New York; 2015. 243–250 p.
53. Saenz-Méndez P, Eriksson LA. Exploring Polypharmacology in Drug Design. In: Mavromoustakos T, Kellici TF (eds.). Rational Drug Design. New York, NY: Springer New York; 2018. 229–243 p.
54. Valdés-Tresanco MS, Valdés-Tresanco ME, Valiente PA, Moreno E. AMDock: a versatile graphical tool for assisting molecular docking with Autodock Vina and Autodock4. Biol Direct. 2020; 15(1): 1–12.
55. Li JJ. Name reactions: a collection of detailed mechanisms and synthetic applications. (5th ed.). Springer Science & Business Media; 2014. 704 p.
56. Nandiyanto ABD, Oktiani R, Ragadhita R. How to Read and Interpret FTIR Spectroscope of Organic Material. Indonesian J Sci Technol. 2019; 4(1): 97–118.
57. Revelou PK, Kokotou MG, Pappas CS, Constantinou-Kokotou V. Direct Determination of Total Isothiocyanate Content in Broccoli Using Attenuated Total Reflectance Infrared Fourier Transform Spectroscopy. J Food Compos Anal. 2017; 61(Special Issue on "Bioactive Sulfur Compounds in Foods: Identification, Quantification and Health Effects"): 47–51.
58. Ngadiwiyana N. Polimerisasi Eugenol Dengan Katalis Asam Sulfat Pekat. J Kim Sains Apl. 2005; 8(2): 43–47.
59. Rahim EA. Synthesis of Soluble Novel Polyacetylenes Containing Carbamate and Eugenol Moieties. Indones J Chem. 2020; 20(4): 818–824.
60. Rahim E, Sanda F, Masuda T. Synthesis and Properties of Novel Eugenol-based Polymers. Polym Bull. 2004; 52(2): 93–100.
61. Pouton CW. Formulation of Poorly Water-Soluble Drugs for Oral Administration: Physicochemical and Physiological Issues and the Lipid Formulation Classification System. Eur J Pharm Sci. 2006; 29(3–4): 278–287.
62. George M, Ghosh I. Identifying the correlation between drug/stabilizer properties and critical quality attributes (CQAs) of nanosuspension formulation prepared by wet media milling technology. Eur J Pharm Sci. 2013; 48(1–2): 142–152.
63. Emami S, Jouyban A, Valizadeh H, Shayanfar A. Are Crystallinity Parameters Critical for Drug Solubility Prediction? J Solution Chem. 2015; 44(12): 2297–2315.
64. Hammoudi R, Sanon S, Mahammed MH. *In vitro* antiplasmodial and cytotoxic properties of some medicinal plants from western Burkina Faso. J Bio Env Sci. 2018; 12(1): 1–4.
65. Hoyer D, Boddeke HWGM. Partial agonists, full agonists, antagonists: dilemmas of definition. Trends Pharmacol Sci. 1993; 14(7): 270–275.
66. Lambert D. Drugs and receptors. BJA Educ. 2004; 4(6): 181–184.
67. Neubig RR, Spedding M, Kenakin T, Christopoulos A. International Union of Pharmacology Committee on Receptor Nomenclature and Drug Classification. XXXVIII. Update on Terms and Symbols in Quantitative Pharmacology. Pharmacol Rev. 2003; 55(4): 597–606.
68. Quesne MG, Ward RA, de Visser SP. Cysteine Protease Inhibition by Nitrile-Based Inhibitors: A Computational Study. Front Chem. 2013; 1(39): 1–10.
69. García-Godoy MJ, López-Camacho E, García-Nieto J, Del Ser J, Nebro AJ, Aldana-Montes JF. Bio-inspired optimization for the molecular docking problem: State of the art, recent results and perspectives. Appl Soft Comput. 2019; 79(6): 30–45.
70. Arianie L, Hermanto FE, Iftitah ED, Warsito W, Widodo N. Novel Antimalarial Drug Screening Based on Methyl Eugenol, Cinnamaldehyde, and Thiosemicarbazone with Cysteine Protease Inhibition: In Silico Molecular Docking, Molecular Dynamics, and ADMET Studies. J Pure Appl Chem Res. 2022; 11(2): 102–112.
71. Daina A, Michielin O, Zoete V. Swissadme: A Free Web Tool to Evaluate Pharmacokinetics, Drug-Likeness and Medicinal Chemistry Friendliness of Small Molecules. Sci Rep. 2017; 7(42717): 1–13.
72. Tripathi P, Ghosh S, Talapatra SN. Bioavailability prediction of phytochemicals present in *Calotropis procera* (Aiton) R. Br. by using Swiss-ADME tool. World Sci News. 2019; 131(5): 147–163.